Journal of Alloys and Compounds 589 (2014) 213–217

Contents lists available at ScienceDirect

Journal of Alloys and Compounds

journal homepage: www.elsevier.com/locate/jalcom

Dispersion of the second harmonic generation in GaN_xAs_{1-x} (x = 0.25, 0.5, 0.75) alloys

A.H. Reshak [a,b,*]

[a] New Technologies – Research Center, University of West Bohemia, Univerzitni 8, 306 14 Pilsen, Czech Republic
[b] Center of Excellence Geopolymer and Green Technology, School of Material Engineering, University Malaysia Perlis, 01007 Kangar, Perlis, Malaysia

ARTICLE INFO

Article history:
Received 24 August 2013
Received in revised form 24 November 2013
Accepted 25 November 2013
Available online 1 December 2013

Keywords:
Semiconductors
Optical materials and properties
Simulation and modelling
Electronic materials
Solar energy materials

ABSTRACT

The all-electron full-potential linearized augmented plane wave method has been used for an *ab initio* theoretical study to investigate the effect of vary the concentration of nitrogen on the second harmonic generation (SHG) of GaN_xAs_{1-x} (x = 0.25, 0.5, 0.75) alloys. Based on the density functional theory the nonlinear optical susceptibilities (NLO) namely the SHG are calculated and their spectra are analyzed. We find that reducing N concentration leads to reduce the energy band gap resulting in enhancing the functionality of GaN_xAs_{1-x} alloys and hence increasing the second-order susceptibility. A surprising finding is a nonlinear relationship between the composition and the absorption/emission energies, leading to significantly enhancing the properties not obtainable from the parent GaAs and GaN binary systems.

1. Introduction

Doping GaAs by a low concentration of nitrogen is found to have a dramatic effect on electronic structure and optical properties of these compounds. GaN_xAs_{1-x} have attracted a great deal of interest due to their unusual physical properties, potential technological importance, the great significance in potential applications such as optoelectronic, semiconductor lasers, and optical detectors [1–5]. Weyers et al. [6] have observed a huge reduction in the band gap that reaches about 0.2 eV by replacing just one percent of the arsenic by nitrogen. The band gap is characterized also by a huge bowing that reaches 18–20 eV for N concentration less than 5%, which is about an order of magnitude larger than other III–V ternary alloys that exhibit a bowing of about 1.0 eV [7,8]. The reason behind the huge bowing parameter of GaN_xAs_{1-x} that is strongly redshifted with increasing nitrogen concentration has been interpreted differently.

Although there have been numerous calculations of the electronic structure and linear optical properties using different methods, to our knowledge there is no experimental data or/and theoretical calculation for the nonlinear optical properties (NLO) of the GaN_xAs_{1-x} alloys appear in the literatures. As natural extension to our previous study [9,10] of the theoretical investigation of the electronic and linear optical properties of GaN_xAs_{1-x}, we thought it would be worthwhile to investigate the effect of vary N concentration in GaN_xAs_{1-x} alloys on the NLO susceptibilities namely the second harmonic generation (SHG) using full potential method [11]. This fact may be used in the future for molecular engineering of the crystals. Since the NLO susceptibilities of these alloys have not been measured or calculated yet. Hence, our study is considered as a quantitative theoretical prediction for such properties, and it still awaits experimental confirmation.

2. Computational method

Self-consistent calculations using a relativistic full-potential linearized augmented plane wave (FP-LAPW) method were carried using the WIEN2K package [11] within Engel–Vosko (EVGGA) scheme [12]. For this, a satisfactory degree of convergence was achieved by considering a number of FP-LAPW basis functions up to R_{MT} K_{max} = 7.0 (where RMT is the minimum radius of the muffin-tin spheres and K_{max} gives the magnitude of the largest k vector in the plane wave expansion). In order to keep the same degree of convergence for all the lattice constants studied, we kept the values of the sphere radii and K_{max} constant over all the range of lattice spacing considered. However, Fourier expanded charge density was truncated at G_{max} = 14(Ryd)$^{1/2}$. We have used the 'special quasi-random structures' (SQS) approach of Zunger et al. [13] to reproduce the randomness of the alloys for the first few shells around a given site. For the composition x = 0.25 and 0.75 the simplest structure is an eight-atom simple cubic lattice (luzonite): the cations with the lower concentration form a regular simple cubic lattice. For x = 0.5, the smallest ordered structure is (0 0 1) supercell. The muffin-tin radii for the composition x = 0.25 and 0.75 are 1.95, 1.9 and 1.6 atomic units (a.u.) for Ga, As and N respectively. Whereas for the composition x = 0.5 a 2.14 a.u. is used for Ga, N and As. The irreducible wedge of the Brillouin zone was described by a mesh of 35 special k-points for binary and ternary alloys except for the case of x = 0.5, where we used a mesh of 64

* Corresponding author at: New Technologies – Research Center, University of West Bohemia, Univerzitni 8, 306 14 Pilsen, Czech Republic. Tel.: +420 777 729 583.
E-mail address: maalidph@yahoo.co.uk

0925-8388/$ - see front matter © 2013 Elsevier B.V. All rights reserved.
http://dx.doi.org/10.1016/j.jallcom.2013.11.175

special k-points. In the case of NLO calculation, we used denser meshes of 10,000 k-points for the ternary alloys of $x = 0.25$, 0.50 and 0.75. The self-consistent calculations are converged since the total energy of the system is stable within 10^{-5} Ry.

3. Optoelectronic properties

3.1. Second harmonic generation

The ternary alloys of GaN_xAs_{1-x} ($x = 0.25$, 0.5, 0.75) possesses cubic structure, the symmetry allows only one nonzero component namely; $\chi^{(2)}_{123}(-2\omega;\omega;\omega)$ [14]. In the first order responses (linear responses) functions, only the interband terms appear and involve only the square of matrix elements, which ensures, for example that $\varepsilon_2(\omega)$ is positive. The second harmonic response involves 2ω resonance in addition to the ω resonance. Thus the matrix element effects are much stronger in nonlinear case. The real and imaginary parts of the products of matrix elements that control the strength of a given resonance in $\chi^{(2)}_{ijk}(-2\omega;\omega;\omega)$ can be positive or negative. The imaginary and real parts of $\chi^{(2)}_{123}(-2\omega;\omega;\omega)$ for the ternary alloys of GaN_xAs_{1-x} is shown in Fig. 1. We should emphasize that increasing N concentration leads to reduce the amplitude and shift all the structures of $\chi^{(2)}_{123}(-2\omega;\omega;\omega)$ towards higher energies, indicated that increasing N concentration leads to reduce the SHG value. Following Fig. 2 one can see that the $\left|\chi^{(2)}_{123}(0)\right|$ values increases from 2.5 to 7.0 to 16.0 to 30.0 to 45.0 pm/V with reducing the N content in GaN_xAs_{1-x} ($x = 1.0$, 0.75, 0.5, 0.25, 0.0) alloys. That is attributed to the fact that the NLO properties are more sensitive to small changes in the band structure than the linear optical properties since the second harmonic response involves 2ω resonance in addition to the usual ω resonance and the threshold for 2ω parts occurs at the half energy of the threshold for ω part, as a result, only the 2ω inter/intra terms contributes to $\chi^{(2)}_{123}(-2\omega;\omega;\omega)$ in the energy range below the fundamental band gap. In Fig. 3, we show $2\omega/\omega$ inter-/intra-band contributions to the total Im $\chi^{(2)}_{123}(-2\omega;\omega;\omega)$. It is clear that the imaginary part of the SHG is zero below half the band gap. The 2ω terms begin to contribute at energies $\sim 1/2E_g$ and the ω terms for energy values above E_g.

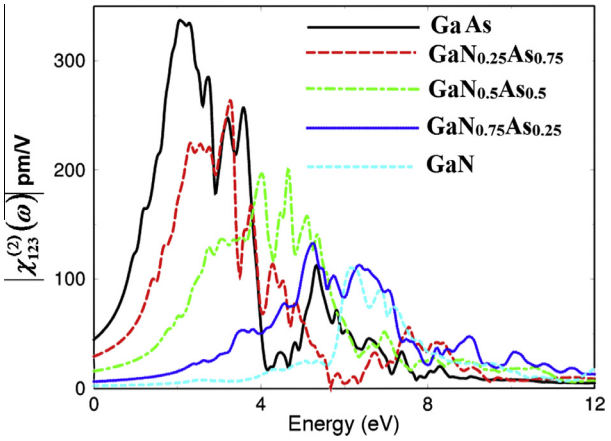

Fig. 2. Calculated $\left|\chi^{(2)}_{123}(-2\omega;\omega;\omega)\right|$ for GaAs, $GaN_{0.25}As_{0.75}$, $GaN_{0.5}As_{0.5}$, $GaN_{0.75}As_{0.25}$ and GaN.

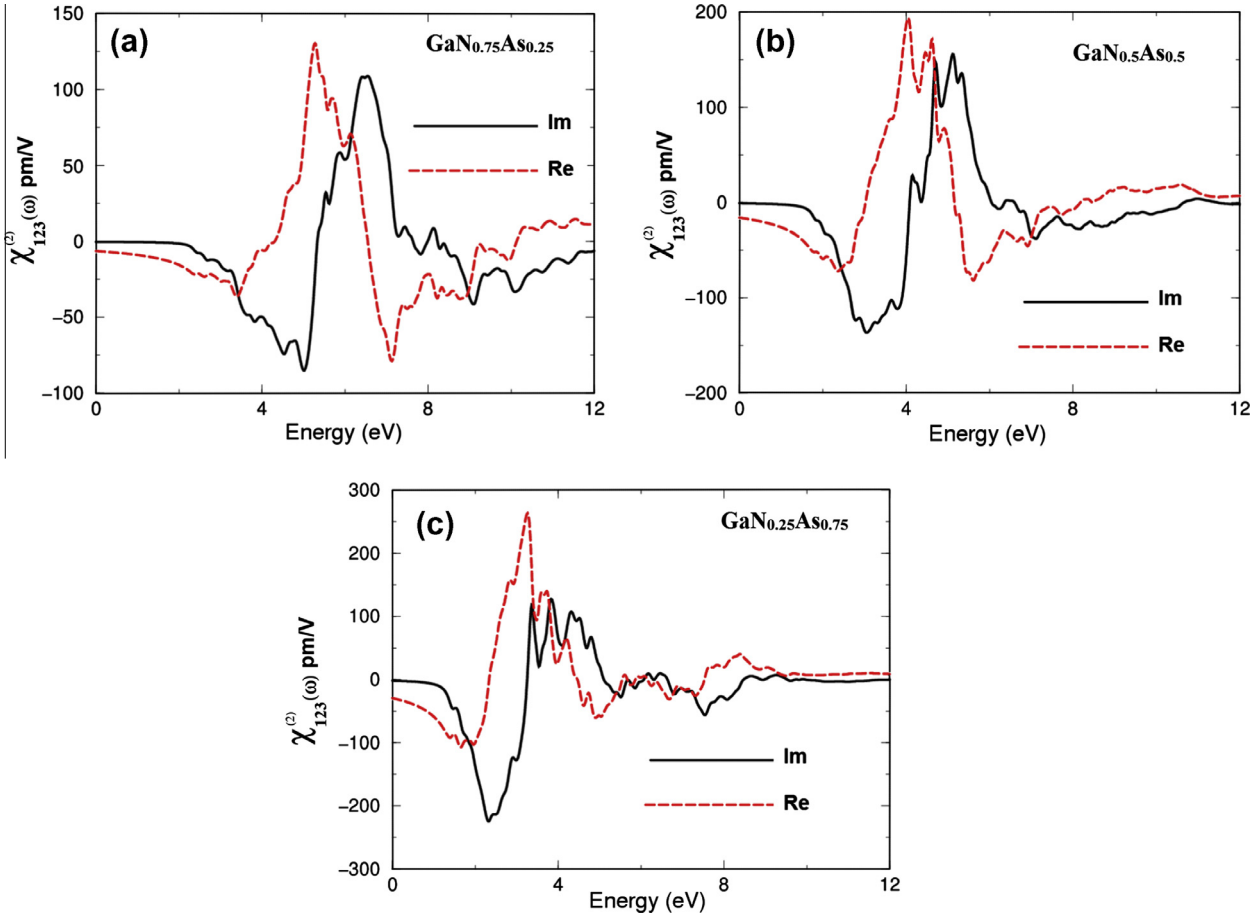

Fig. 1. Calculated imaginary and real parts for (a) $GaN_{0.75}As_{0.25}$, (b) $GaN_{0.5}As_{0.5}$, (c) $GaN_{0.25}As_{0.75}$.

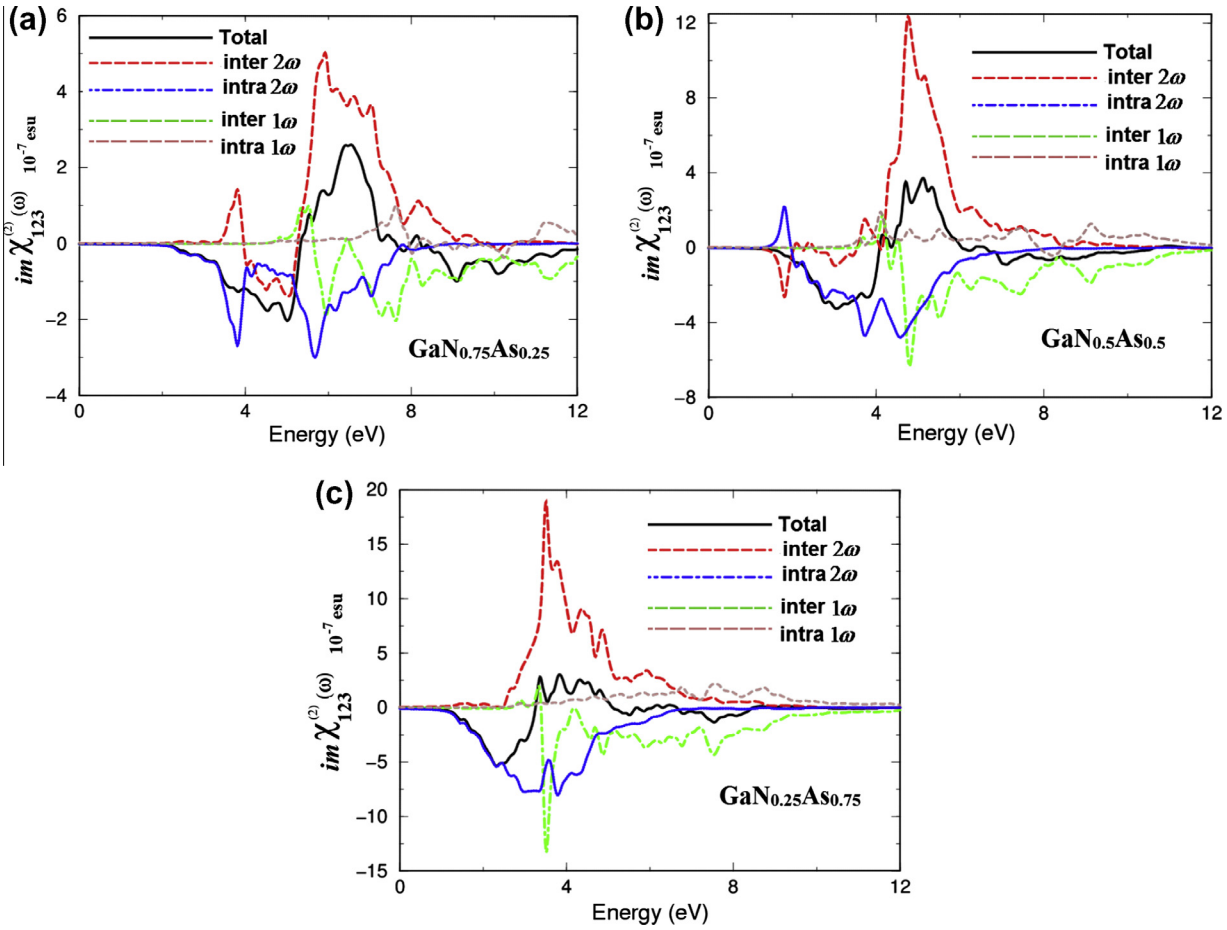

Fig. 3. Calculated total $\left|\chi^{(2)}_{123}(-2\omega;\omega;\omega)\right|$ spectrum (dark solid curve-black) along with the intra $(2\omega)/(1\omega)$ (light solid curve-blue)/(light dashed doted curve-cyan) and inter $(2\omega)/(1\omega)$ (light long dashed curve-red)/(light doted curve-green)-band contributions, here all $\left|\chi^{(2)}_{123}(-2\omega;\omega;\omega)\right|$ are multiplied by 10^{-7}, in esu units; for; (a) $GaN_{0.75}As_{0.25}$, (b) $GaN_{0.5}As_{0.5}$, (c) $GaN_{0.25}As_{0.75}$. (For interpretation of the references to colour in this figure legend, the reader is referred to the web version of this article.)

At low spectral range (⩽half the fundamental band gap) the SHG optical spectra is dominated by 2ω contributions. Beyond the fundamental band gap the major contribution comes from ω term.

One would expect that the spectral structures in Im $\chi^{(2)}_{123}(-2\omega;\omega;\omega)$ could be understood from the structures in $\varepsilon_2(\omega)$. Unlike the linear optical spectra, the features in the SHG are more difficult to identify from the band structure, because of the presence of 2ω and ω terms. But we can make use of the linear optical spectra to identify the different resonance leading to various features in the SHG spectra. The first structure in Im $\chi^{(2)}_{123}(-2\omega;\omega;\omega)$, between 0.0 and 4.0 eV is primarily originates from 2ω resonance and arise from the first structure in $\varepsilon_2(\omega)$. The second structure between 4.0 and 8.0 eV is associated with interference between a ω resonance and 2ω resonance and associated with high structure in $\varepsilon_2(\omega)$. The last structure from 8.0 – 12.0 eV is mainly due to ω resonance and associated with the tail in $\varepsilon_2(\omega)$. We can identify the origin of the spectral peaks in the figures as caused by $2\omega/\omega$ inter-intra-band contributions in the linear dielectric function. To analyze the features of the calculated $\chi^{(2)}_{123}(-2\omega;\omega;\omega)$ spectra, it would be worthwhile to compare the absolute value of $|\chi^{(2)}_{123}(-2\omega;\omega;\omega)|$ component (Fig. 4 – upper panel) with the absorptive part of the corresponding dielectric function $\varepsilon_2(\omega)$ as a function of both $\omega/2$ and ω (Fig. 4 – lower panel). The first structure $\left|\chi^{(2)}_{123}(-2\omega;\omega;\omega)\right|$ between 0.0 and 4.0 eV is mainly originated from 2ω resonance (see $\varepsilon_2(\omega/2)$ Fig. 4 – lower panel). The second structure between 4.0 and 8.0 eV is associated with interference between 2ω and ω resonances (the threshold of $\varepsilon_2(\omega)$) (see $\varepsilon_2(\omega/2)$ and $\varepsilon_2(\omega)$ Fig. 4 – lower panel). The last spectral structure (within 8.0–12.0 eV) is mainly due to ω resonance and is associated with the second structure in $\varepsilon_2(\omega)$.

To the best of our knowledge there is no experimental data for NLO susceptibilities of the ternary alloys ($GaN_{0.75}As_{0.25}$, $GaN_{0.5}As_{0.5}$, and $GaN_{0.25}As_{0.25}$) are available in the literatures to compare with our theoretical results. We would like to mention here that in our previous works [14–21] we have calculated the linear and nonlinear optical susceptibilities using FPLAPW method on several systems whose linear and nonlinear optical susceptibilities are known experimentally. We find very good agreement with the experimental data. Thus we believe that our calculations reported in this paper would produce very accurate and reliable results.

4. Conclusion

We have performed first principle calculations of the NLO susceptibilities namely the SHG of GaN_xAs_{1-x} ($x = 0.25, 0.5, 0.75$) alloys within a framework of FP-LAPW method. The evaluations are based on the calculations of the energy band structure. The analysis of our calculations confirms the enhancement of the functionality of the SHG of GaN_xAs_{1-x} ($x = 0.25, 0.5, 0.75$) alloys with vary N concentration. Calculations are reported for the spectral features of the SHG and its static limit. We note that reducing N concentration in GaN_xAs_{1-x} ($x = 1.0, 0.75, 0.5, 0.25, 0.0$) alloys leads to significantly enhance the second-order susceptibility from 2.5 to

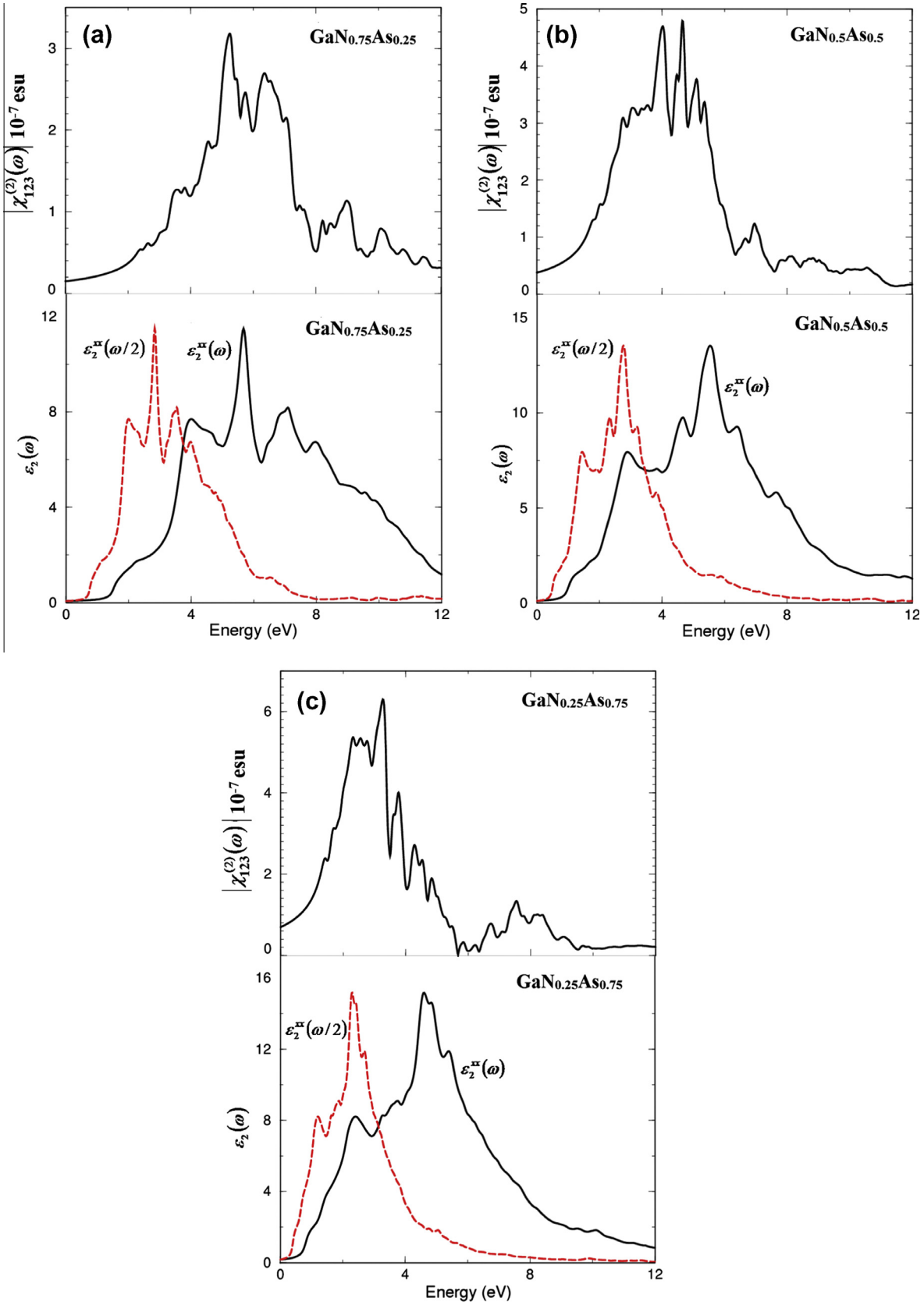

Fig. 4. –*upper panel* – Calculated $\left|\chi^{(2)}_{123}(-2\omega;\omega;\omega)\right|$ (dark solid curve-black); – *lower panel*–Calculated $\varepsilon_2^{xx}(\omega)$ (dark solid curve-black color online); calculated $\varepsilon_2^{xx}(\omega/2)$ (dark dashed curve-red) for (a) $GaN_{0.75}As_{0.25}$, (b) $GaN_{0.5}As_{0.5}$, (c) $GaN_{0.25}As_{0.75}$. (For interpretation of the references to colour in this figure legend, the reader is referred to the web version of this article.)

7.0 to 16.0 to 30.0 to 45.0 pm/V, respectively. This fact may be used in the future for molecular engineering of the crystals. To the best of our knowledge, the nonlinear optical properties of these compounds have not been measured or calculated yet. Hence, our study is considered as a quantitative theoretical prediction for such properties, and it still awaits experimental confirmation.

Acknowledgements

The result was developed within the CENTEM project, reg. no. CZ.1.05/2.1.00/03.0088, co-funded by the ERDF as part of the Ministry of Education, Youth and Sports OP RDI programme. School of Material Engineering, Malaysia University of Perlis, Malaysia.

References

[1] J.W. Orton, C.T. Foxon, Rep. Prog. Phys. 61 (1918) 1–75.
[2] S.C. Jain, M. Willander, J. Narayan, R. Van Overstraeten, J. Appl. Phys. 87 (2000) 965–997.
[3] I. Vurgaftman, J.R. Meyer, J. Appl. Phys. 94 (2003) 3675–3697.
[4] H.P. Xin, C.W. Tu, Appl. Phys. Lett. 72 (1998) 2442–2444.
[5] W. Shan, W. Walukiewicz, J.W. Ager III, E.E. Haller, J.F. Geisz, D.J. Friedman, J.M. Olson, S.R. Kurtz, Phys. Rev. Lett. 82 (1999) 1221–1224.
[6] M. Weyers, M. Sato, H. Ando, Jpn. J. Appl. Phys. 31 (1992) L853–L855.
[7] M. Kondow, K. Uomi, K. Hosomi, T. Mozume, Jpn. J. Appl. Phys. 33 (1994) L1056–L1058.
[8] S. Sakai, Y. Ueta, Y. Terauchi, Jpn. Appl. Lett. 32 (1993) 4413–4417.
[9] A.H. Reshak, Z. Charifi, H. Baaziz, Sol. Energy 90 (134–4) (2013) 3.
[10] H. Baaziz, Z. Charifi, A.H. Reshak, B. Hamad, Y. Al-Dori, Appl. Phys. A 106 (2012) 687–696.
[11] P. Blaha, K. Schwarz, G.K.H. Madsen, D. Kvasnicka, J. Luitz, WIEN2K, An Augmented Plane Wave Plus Local Orbitals Program for Crystal Properties, Vienna University of Technology, Vienna, Austria, 2001.
[12] E. Engel, S.H. Vosko, Phys. Phys. Rev. B 47 (1993) 13164–13174.
[13] A. Zunger, S.-H. Wei, L.G. Feireira, J.E. Bernard, Phys. Rev. Lett. 65 (1990) 353–356.
[14] A.H. Reshak, J. Chem. Phys. 124 (2006) 104707–104712;
A.H. Reshak, J. Chem. Phys. 125 (2006) 034710–034718.
[15] A.H. Reshak, I.V. Kityk, S. Auluck, J. Phys. Chem. B 114 (2010) 16705–16712.
[16] A.H. Reshak, Eur. Phys. J. B 47 (2005) 503–508.
[17] A.H. Reshak, S. Auluck, I.V. Kityk, J. Phys. Condens. Matter 20 (2008) 145209.
[18] A.H. Reshak, S. Auluck, Dalibor Stys, I.V. Kityk, H. Kamarudin, J. Berdowski, Z. Tylczynskif, J. Mater. Chem. 21 (2011) 17219.
[19] A.H. Reshak, M. Piasecki, S. Auluck, I.V. Kityk, R. Khenata, B. Andriyevsky, C. Cobet, N. Esser, A. Majchrowski, M. Ś wirkowicz, R. Diduszko, W. Szyrski, J. Phys. Chem. B. 113 (2009) 46.
[20] A.H. Reshak, Xuean Chen, S. Auluck, H. Kamarudin, Jan Chyský A. Wojciechowski, I.V. Kityk, J. Phys. Chem. B. 117 (2013) 14141–14150.
[21] A.H. Reshak, Y.M. Kogut, A.O. Fedorchuk, O.V. Zamuruyeva, G.L. Myronchuk, O.V. Parasyuk, H. Kamarudin, S. Auluck, K.J. Plucinskig, Jiri Bilah, Phys. Chem. Chem. Phys. 15 (2013) 18979.